Penerbit Akademia Baru

Journal of Advanced Research Design

Journal homepage:
https://akademiabaru.com/submit/index.php/ard
ISSN: 2289-7984

Metaheuristic Optimization of Perovskite Solar Cell Using Hybrid L_{32} Taguchi Doe-Based Genetic Algorithm

Khairil Ezwan Kaharudin[1,2], Nabilah Ahmad Jalaludin[1], Fauziyah Salehuddin[1,*], Faiz Arith[1], Anis Suhaila Mohd Zain[1], Ibrahim Ahmad[3], Siti Aisah Mat Junos[1], Prakash R Apte[4]

[1] Micro & Nano Electronics (MiNE), CeTRI, Faculty of Electronics and Computer Technology and Engineering, Universiti Teknikal Malaysia Melaka, Hang Tuah Jaya, Durian Tunggal, 76100 Melaka, Malaysia
[2] Faculty of Engineering and Built Environment, Lincoln University College (Main Campus), Wisma Lincoln, 47301 Petaling Jaya, Selangor, Malaysia
[3] College of Engineering (CoE), Universiti Tenaga Nasional (UNITEN), 43009 Kajang, Selangor, Malaysia
[4] Indian Institute of Technology (IIT), Bombay, Powai, Mumbai 400076, India

ARTICLE INFO

Article history:
Received 21 March 2024
Received in revised form 23 August 2024
Accepted 19 September 2024
Available online 30 November 2024

Keywords:
Genetic algorithm; L_{32} Taguchi DoE; multiple linear regression; power conversion efficiency

ABSTRACT

Solar cells convert sunlight into electricity, and the efficiency of this conversion process largely depends on the material parameters. Optimizing these parameters, like thickness and carrier concentration, could significantly increase the efficiency of solar cells. This paper emphasizes the metaheuristic optimization approach in searching for the optimum input parameters of perovskite solar cell (PSC). The proposed approach is realized using Solar Cell Capacitance Simulator (SCAPS-1D) software incorporated with a hybrid L_{32} Taguchi DoE-based Genetic Algorithm. Based on Multiple Linear Regression (MLR) analysis, the thickness of mix halide perovskite ($CH_3NH_3PbI_{3-x}Cl_x$) was discovered to be the most crucial input parameter affecting the Power Conversion Efficiency (PCE) variations. Based on the result of the Genetic algorithm, the optimal values of the input parameters: Fluorine doped tin oxide (FTO) thickness, FTO donor density, Titanium Dioxide (TiO_2) layer thickness, TiO_2 donor density, $CH_3NH_3PbI_{3-x}Cl_x$ layer thickness, $CH_3NH_3PbI_{3-x}Cl_x$ donor density, graphene oxide (GO) layer thickness, and GO acceptor density are predicted to be 0.187 µm, 9.965×10^{21} cm^{-3}, 0.033 µm, 9.629×10^{21} cm^{-3}, 0.926 µm, 9.983×10^{21} cm^{-3}, 0.039 µm and 9.671×10^{21} cm^{-3} respectively. Using the predicted optimum input parameters, the simulation generates the best value of open voltage (Voc), current density (Jsc), fill factor (FF), and PCE measured at 1.647 V, 25.68 mA/cm^2, 92.03%, and 38.93%, respectively.

1. Introduction

The increasing electricity demand results from accelerated industrialization and rising household electricity consumption. Free and environmentally friendly electricity is the optimal solution to these increasing electricity requirements since it is not detrimental to the environment. As one of the most accessible renewable energy sources, solar energy ranks among the most appealing alternatives. It

* *Corresponding author.*
E-mail address: fauziyah@utem.edu.my

https://doi.org/10.37934/ard.122.1.219233

could be one of the most effective solutions to meet increasing electricity demands. Furthermore, solar energy may also be readily turned into electricity, which may be realized by developing solar cells, photovoltaic devices, and solar absorbers, to name a few.

Metamaterials have received much interest due to their distinctive electro-optical properties and tiny size, as opposed to large optical devices. It has been discovered that by utilizing dielectric metamaterials rather than glass, the Perovskite's light conversion efficiency could be increased. Due to excellent power conversion efficiency (PCE), perovskite solar cells (PSCs) have attracted much attention in the field of research [1-5]. Moreover, modern advances in device layouts and material processing features have made PSC manufacturing one of the most promising trends in photovoltaics. The ultimate goal is to improve the architectural layout of the structure and the selection of materials in accordance with the significant performance increase that has forcefully enabled various exploratory and hypothetical evaluations.

The PSCs have an electron transport material (ETM) and a hole transport material (HTM) between a perovskite absorber layer. Note that electrons and holes, two types of carriers, are produced when light is absorbed. Carriers move via a transporting channel after being stimulated by an incident photon. Therefore, it goes without saying that the absorber-to-front/back electrode carrier route significantly affects the PCE [6-9]. In order to further increase the PCE of PSC, the scientific community has recently focused a great deal of emphasis on introducing novel materials in the aforementioned route, particularly in the ETM, HTM, and absorber [10-13].

Design of Experiments (DoE) is a statistical approach for recognizing multiple input parameters and interactions that significantly impact the output of a device/system/process. In simulation modeling, DoE can assist in identifying essential factors with minimal simulation [14-17]. Furthermore, randomization, replication of experimental trials, and division are unnecessary in simulation-based DoE since the deterministic trait of simulations hinders experimental variation. Metaheuristics are advanced algorithms tailored for finding, creating, or choosing partial search algorithms (heuristics) that can yield reasonably effective solutions for complex optimization problems, particularly under conditions of incomplete data or limited computational resources [18-23]. They leverage learning from previous solutions to more effectively navigate the solution space. Applied extensively in sectors such as business, engineering, economics, and science, metaheuristics tackle complex problems that defy easy resolution through conventional methods. While they don't assure the best solution, their goal is to identify viable solutions efficiently. Motivated by the impact of multiple layer variations on the PCE, this work aims to simulate and optimize multiple layers of PSC using a proposed hybrid L_{32} Taguchi DoE-based Genetic Algorithm. The primary contributions of this research work are listed below:

i. We have analyzed and studied the impact of layer parameters of the PSC towards PCE. We have discovered that the thickness of the perovskite (CH3NH3PbI3-XClX) layer is the most significant input parameter contributing to the considerable variance in the PCE.
ii. We have optimized and predicted the optimum layer parameters of the PSC that generate the highest possible PCE. We have successfully simulated a PSC model that generates 38.93% of PCE.

2. Related Works

L_8 Taguchi DoE was utilized to optimize input parameters in silicon-based solar cell simulation [24]. The findings demonstrate that an energy of 10 keV combined with a boron density of 5.0 x 10^{15} cm^{-3} and phosphorus density of 2.0 x 10^{16} cm^{-3} yields a junction depth of 0.3 x 0.5 um and a stable FF

value of 80%, with PCE of 15% to 16%. The PCE of the silicon-based solar cell increased by 1% due to the optimized boron and phosphorus densities predicted using the L_8 Taguchi DoE. For higher PCE in Dye Solar Cell (DSC) fabrication, the L_8 Taguchi DoE was employed as well to optimize material thickness, surface area, and material density in electrolytes [25]. The proposed device suggests an optimum DSC efficiency of 4.59165% can be achieved using the optimized material's thickness and density. The results clearly indicate the optimum efficiency of the DSC device could be attained by predicting the most optimum thickness and density of the applied materials.

Response surface methodology (RSM) DoE was used to obtain the best PCE as the thickness was predictively tuned at 5 µm and 50 µL graphene quantum dots (GQD) [26]. The L_9 Taguchi DoE was used in conjunction with the Analysis of Microelectronic and Photonic Structures (AMPS-1D) software to model a PSC device [27]. The findings revealed that Cadmium Sulphide (CdS) and Copper Telluride (CuTe) were deemed marginally significant on PCE, with the device demonstrating significantly enhanced PCE. The L_9 Taguchi DoE was employed as well to optimize dye sensitised solar cell fabrication, with the experimental findings revealing that magnesium nitrate concentration had the greatest influence on photocurrent densities, followed by deposition time [28].

Solar Cell Capacitance Simulator (SCAPS-1D) software was used in conjunction with the L_9 Taguchi DoE to optimize the absorber layer grading profile on the Copper Indium Gallium Selenide (CIGS) photovoltaic cell's properties. The results demonstrated that an average PCE of 22.08% using the optimized absorber layer grading profile [29]. The PCE of a tandem organic solar cell was optimized using RSM DoE [30]. In comparison to the conversion rate of the monolayer solar cell using the same materials, the optimized thicknesses increased the PCE by 47.7%.

The RSM DoE was also used to examine the impact of coating silicon solar cells with zinc oxide, aluminum oxide, titanium dioxide on their overall optical performance [31]. Applying ZnO material with a thickness of 38 nm, the research establishes the optimal conditions of silicon solar cell with reduced surface reflections. For the first time, the parameters of the triple diode model (TDM) of PSCs were determined using an improved version of the bald eagle search optimization method [32]. The results highlight the advantages of the improved version of the bald eagle search optimizer when compared to other methods, including the original bald eagle search optimization, particle swarm in optimization, hunger games search, and the latest coronavirus disease optimization algorithm in which it produced the highest current density of the PSC.

In our study, we have applied a hybrid metaheuristic optimization in modelling multiple layer parameters of PSC device using SCAPS-1D with a hybrid L_{32} Taguchi DoE-based Genetic Algorithm for an improved PCE. Additionally, we evaluated the PCE from our proposed approach against the PCE derived solely from the L_{32} Taguchi DoE for conclusive comparison.

3. Methodology

Proposed methodology of this work comprises four stages; Simulation of Perovskite solar cell, L_{32} Taguchi Design of Experiments (DoE), Multiple Linear Regression and Genetic algorithm. The proposed flowchart of the methodology are depicted in Figure 1.

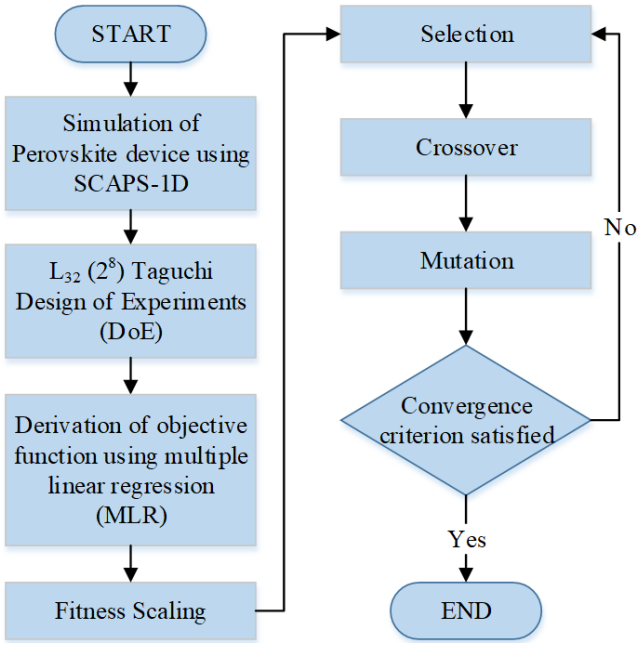

Fig. 1. Flowchart of the methodology

3.1 Perovskite Solar Cell Simulation

A perovskite solar cell configuration was studied, with graphene oxide (GO) used as hole transport material (HTM) to prevent electron flow. The Solar Cell Capacitance Simulator (SCAPS-1D) was used to build the whole device assembly shown in Figure 2. Figure 3 shows the energy band diagram of the proposed perovskite device structure. In order to simulate the current-voltage characteristics of the device, appropriate values of layer parameters were inserted. Table 1 shows multiple physical parameters used in this work.

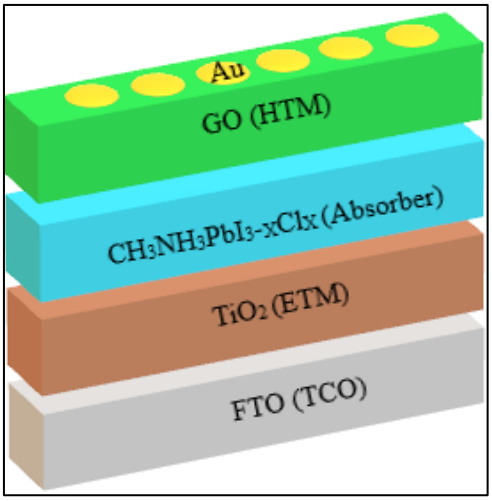

Fig. 2. Perovskite device structure

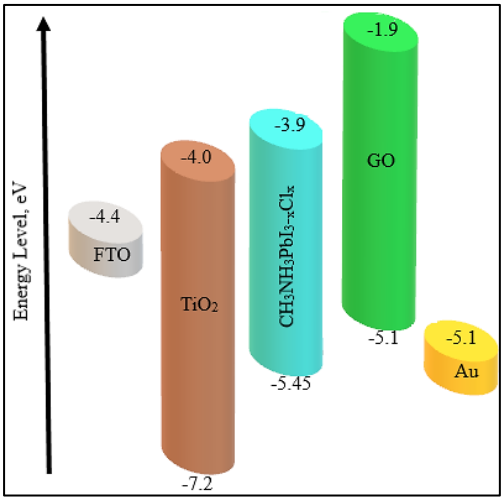

Fig. 3. Energy band diagram of Perovskite device structure

The main function of GO layer is to promote carrier accumulation at the metallic electrode. Furthermore, the degradation of a perovskite device could be lowered by reducing ion electro migration from the metallic electrode to the perovskite layer, which triggers electrical shunting. In addition, rapid heat dispersion from the GO layer to the surrounding environment increases the

thermal stability of the perovskite device, hence lowering the volume of heat created within the cell during actual operation. The parameters of GO layer and the perovskite planar layer must be carefully configured, as a large interlayer discrepancy will increase the recombination rate otherwise.

Table 1
Parameters used in the simulation work

Parameter	TCO	ETL	Absorber	HTL
	FTO	TiO_2	$CH_3NH_3PbI_{3-X}Cl_X$	GO
Thickness (µm)	0.1	0.03	0.9	0.05
Bandgap (eV)	3.5	3.2	1.55	3.2
Electron affinity (eV)	4	4	3.9	1.9
Dielectric permittivity (relative)	9	100	6.5	3
Conduction band effective density of states (cm^{-3})	$2.2x10^{18}$	10^{19}	$2.2x10^{17}$	$2.2x10^{21}$
Valence band effective density of states (cm^{-3})	$1.8x10^{19}$	10^{19}	$1.8x10^{19}$	$1.8x10^{21}$
Electron thermal velocity (cm/s)	10^7	10^7	10^7	10^7
Hole thermal velocity (cm/s)	10^7	10^7	10^7	10^7
Electron mobility (cm^2/Vs)	20	$6x10^{-3}$	2	100
Hole mobility (cm^2/Vs)	10	$6x10^{-3}$	2	300
Shallow uniform donor density, N_D (cm^{-3})	10^{19}	10^{19}	10^{17}	-
Shallow uniform acceptor density, N_A (cm^{-3})	-	-	-	10^{20}
Defect density, N_t (cm^{-3})	10^{15}	10^{15}	10^{13}	10^{15}
References	[33]	[33]	[33]	[34]

The GO layer was employed as planar structure as was suggested in previous researches [34-36]. SCAP-1D was used to simulate the electrical characteristics of the perovskite cell, which were initially displayed in Figure 4. During numerical simulation, a typical solar spectrum AM 1.5 is projected to the front contact in which the carrier transport, drift-diffusion, and recombination models are computed to extract open circuit voltage (Voc), short circuit current density (Jsc), fill factor (FF), and power conversion efficiency (PCE) of the perovskite device.

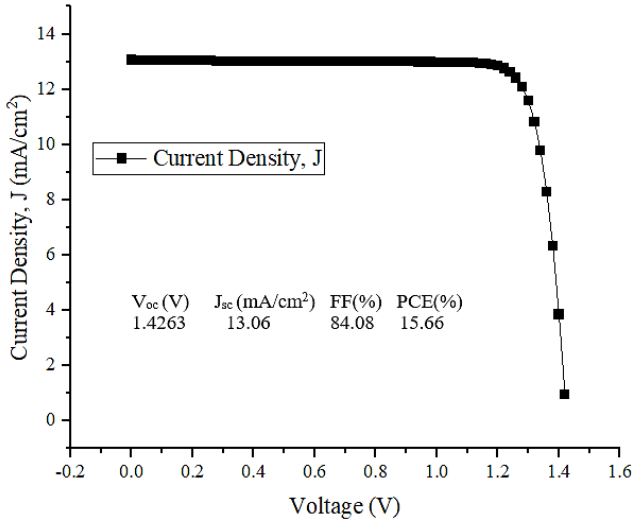

Fig. 4. Initial current–voltage characteristics of PSC

3.2 L_{32} Taguchi Design of Experiments (DoE)

Taguchi DoE employs specific orthogonal arrays to investigate all design parameters with the least number of tests. In this work, L_{32} Taguchi DoE shown in Table 2, is utilized to attain corresponding

power conversion efficiency (PCE) for 32 different experiment sets. Each input parameters are varied into two levels; low and high as listed in Table 3.

Table 2
Input parameters and their levels

Symbol	Input parameter	Unit	Low	High
a	FTO thickness	µm	0.1	0.9
b	FTO donor concentration	cm^{-3}	1E+11	1E+20
c	TiO_2 thickness	µm	0.03	0.09
d	TiO_2 donor concentration	cm^{-3}	1E+11	1E+20
e	$CH_3NH_3PbI_{3-X}Cl_X$ thickness	µm	0.1	0.9
f	$CH_3NH_3PbI_{3-X}Cl_X$ donor concentration	cm^{-3}	1E+11	1E+20
g	GO thickness	µm	0.03	0.09
h	GO acceptor concentration	cm^{-3}	1E+11	1E+20

Table 3
L_{32} Taguchi design of experiments

Exp. No.	Level of input parameters							
	A	B	C	D	E	F	G	H
1	Low	Low	Low	Low	Low	Low	Low	Low
2	Low	Low	Low	Low	High	Low	High	High
3	Low	Low	Low	High	Low	High	Low	High
4	Low	Low	Low	High	High	High	High	Low
5	Low	Low	High	Low	Low	High	High	Low
6	Low	Low	High	Low	High	High	Low	High
7	Low	Low	High	High	Low	Low	High	High
8	Low	Low	High	High	High	Low	Low	Low
9	Low	High	Low	Low	Low	High	High	High
10	Low	High	Low	Low	High	High	Low	Low
11	Low	High	Low	High	Low	Low	High	Low
12	Low	High	Low	High	High	Low	Low	High
13	Low	High	High	Low	Low	Low	Low	High
14	Low	High	High	Low	High	Low	High	Low
15	Low	High	High	High	Low	High	Low	Low
16	Low	High	High	High	High	High	High	High
17	High	Low	Low	Low	Low	High	High	High
18	High	Low	Low	Low	High	High	Low	Low
19	High	Low	Low	High	Low	Low	High	Low
20	High	Low	Low	High	High	Low	Low	High
21	High	Low	High	Low	Low	Low	Low	High
22	High	Low	High	Low	High	Low	High	Low
23	High	Low	High	High	Low	High	Low	Low
24	High	Low	High	High	High	High	High	High
25	High	High	Low	Low	Low	Low	Low	Low
26	High	High	Low	Low	High	Low	High	High
27	High	High	Low	High	Low	High	Low	High
28	High	High	Low	High	High	High	High	Low
29	High	High	High	Low	Low	High	High	Low
30	High	High	High	Low	High	High	Low	High
31	High	High	High	High	Low	Low	High	High
32	High	High	High	High	High	Low	Low	Low

3.3 Multiple Linear Regression

Multiple linear regression is an algorithm for machine learning that predicts a dependable variable based on the magnitude of two or more independent variables. In other words, the independent variables are the parameters through which the dependent variable (response) or outcome is calculated. A multiple regression model extends to numerous explanatory variables. In this work, the multiple linear regression is used to derive the objective function that describe the relationship between a predictor variable and the response. Hence, the objective function that relates eight independent inputs; *a*, *b*, *c*, *d*, *e*, *f*, *g* and *h* with one dependent output; PCE can be written as:

$$PCE = B_0 + B_1 a + B_2 b + B_3 c + B_4 d + B_5 e + B_6 f + B_7 g + B_8 h \quad (1)$$

where B_0 is the y-intercept, $B_1 B_2 B_3 B_4 B_5 B_6 B_7 B_8$ represent the regression coefficients for the corresponding input parameters.

3.4 Genetic Algorithm

Genetic algorithm is an approach for addressing both limited and unbounded optimization based on mechanism that drives evolutionary biology. As depicted in Figure 5, the Genetic algorithm involves numerous phases consisting of initial population, objective function, fitness scaling, selection, crossover, and mutation.

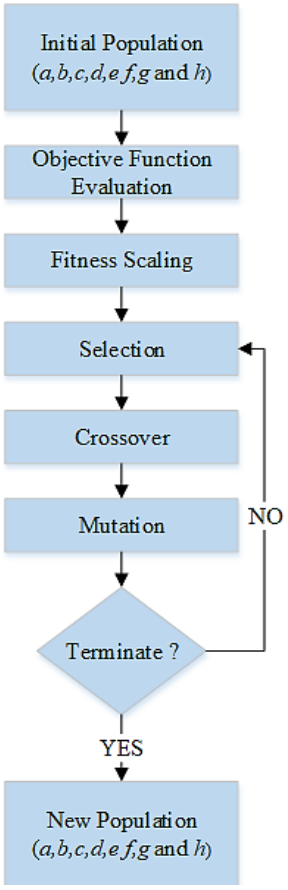

Fig. 5. Process flow of Genetic algorithm

In this study, the initial population consisted of the starting values of FTO thickness, FTO donor density, TiO_2 layer thickness, TiO_2 donor density, $CH_3NH_3PbI_{3-x}Cl_x$ layer thickness, $CH_3NH_3PbI_{3-x}Cl_x$ donor density, GO layer thickness, and GO acceptor density, represented by *a*, *b*, *c*, *d*, *e*, *f*, *g*, and *h*, respectively. The objective function derived by multiple linear regression was then scaled to fit within predetermined lower and upper constraints. Since the primary purpose was to search for the largest value of PCE, the fitness function (f_i) for this objective problem was defined as depicted in Figure 6. The default preferences of Genetic algorithm for this study was shown in Figure 7.

Minimize -$f_i(a, b, c, d, e, f, g, h)$
Subject to the constraints:
$0.05 \leq a \leq 0.95$
$1e+06 \leq b \leq 1e+22$
$0.01 \leq c \leq 0.11$
$1e+06 \leq d \leq 1e+22$
$0.05 \leq e \leq 0.95$
$1e+06 \leq f \leq 1e+22$
$0.01 \leq g \leq 0.11$
$1e+06 \leq h \leq 1e+22$

Fig. 6. Fitness function subjected to the constraints

Type = real-valued
Population size = 50
Number of generations = 1000
Elitism = 2
Crossover probability = 0.8
Mutation probability = 0.1

Fig. 7. Default preferences of Genetic algorithm

4. Results and Discussion

This section discusses the results of metaheuristic optimization for improved PCE of the Perovskite Solar Cell by incorporating L_{32} Taguchi DoE, multiple linear regression, and the Genetic algorithm. Table 4 displays the simulation results in which the PCE values for 32 experimental rows were recorded, accordingly. The relationship between eight layer parameters and the PCE values for 32 experimental rows is subsequently examined using the MLR approach, from which the normal Q-Q plot illustrated in Figure 8 is derived. There are no data in the actual dataset near the center of the theoretical distribution, hence there is no point on the Q-Q plot at this location (0, 0). The top half of the Q-Q plot is a reflection of the lower half across x and y. The residuals are therefore seen as having a bimodal distribution. Table 5 presents the results of the multiple linear regression for this investigation. It is clearly evident that the most significant input parameter contributing the considerable variance on the PCE is input parameter *e* ($CH_3NH_3PbI_{3-X}Cl_X$ thickness) as it exhibits the least p-value among others.

On the other side, the least significant input parameter is recognized as input parameter *g* (GO thickness) since it exhibits the largest p-value among others. In practice, any p-value below 0.05 is typically viewed as significant which imply the coefficient does in fact contribute value to the model by helping to explain the variation within PCE. MLR analysis indicates that GO material has the minimal impact on PCE among the layers. However, GO provides excellent chemical compatibility with perovskite materials, securing stable interfaces and reducing interfacial recombination that can harm device efficiency. The fabrication process for GO is relatively simple and inexpensive, making it a good option for mass production of PSCs. Additionally, GO contributes to the thermal and chemical stability of PSCs, which is critical for their longevity and effectiveness.

Table 4
Simulated PCEs from L_{32} Taguchi DoE

Exp. No.	Level of input parameters								PCE
	A	B	C	D	E	F	G	H	(%)
1	Low	Low	Low	Low	Low	Low	Low	Low	15.66
2	Low	Low	Low	Low	High	Low	High	High	27.85
3	Low	Low	Low	High	Low	High	Low	High	18.30
4	Low	Low	Low	High	High	High	High	Low	34.87
5	Low	Low	High	Low	Low	High	High	Low	17.91
6	Low	Low	High	Low	High	High	Low	High	34.51
7	Low	Low	High	High	Low	Low	High	High	15.56
8	Low	Low	High	High	High	Low	Low	Low	27.45
9	Low	High	Low	Low	Low	High	High	High	18.59
10	Low	High	Low	Low	High	High	Low	Low	35.74
11	Low	High	Low	High	Low	Low	High	Low	15.97
12	Low	High	Low	High	High	Low	Low	High	28.94
13	Low	High	High	Low	Low	Low	Low	High	15.91
14	Low	High	High	Low	High	Low	High	Low	28.20
15	Low	High	High	High	Low	High	Low	Low	18.40
16	Low	High	High	High	High	High	High	High	35.63
17	High	Low	Low	Low	Low	High	High	High	17.22
18	High	Low	Low	Low	High	High	Low	Low	32.76
19	High	Low	Low	High	Low	Low	High	Low	14.65
20	High	Low	Low	High	High	Low	Low	High	26.13
21	High	Low	High	Low	Low	Low	Low	High	14.60
22	High	Low	High	Low	High	Low	High	Low	25.23
23	High	Low	High	High	Low	High	Low	Low	17.15
24	High	Low	High	High	High	High	High	High	32.82
25	High	High	Low	Low	Low	Low	Low	Low	15.79
26	High	High	Low	Low	High	Low	High	High	28.65
27	High	High	Low	High	Low	High	Low	High	18.40
28	High	High	Low	High	High	High	High	Low	35.43
29	High	High	High	Low	Low	High	High	Low	18.07
30	High	High	High	Low	High	High	Low	High	35.27
31	High	High	High	High	Low	Low	High	High	15.65
32	High	High	High	High	High	Low	Low	Low	28.00

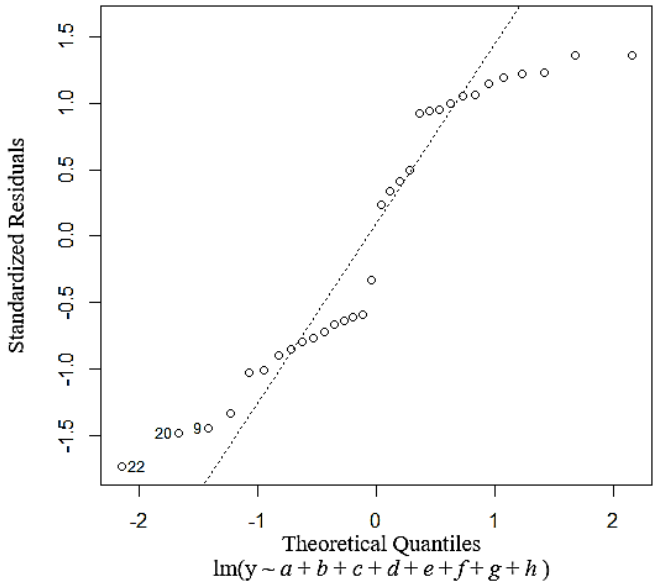

Fig. 8. Normal Q-Q plot

Table 5
Results of the multiple linear regression

Regression coefficients	Estimation	Std. error	t value	Pr (>|t|)	Significant code
Intercept	1.266e+01	1.020	12.404	1.14e-11	***
a	-1.068	6.352e-01	-1.681	0.106	
b	1.248e-20	5.082e-21	2.456	0.022	*
c	-4.781	8.470	-0.565	0.578	
d	8.688e-22	5.082e-21	0.171	0.866	
e	1.794e+01	6.352e-01	28.244	< 2e-16	***
f	4.803e-20	5.082e-21	9.449	2.20e-09	***
g	-7.396e-01	8.47	-0.087	0.931	
h	1.719e-21	5.082e-21	0.338	0.738	
Significant Code: 0 '***', 0.001 '**', 0.01 '*', 0.05 '.' 0.1-1 ' '					
Residual standard error	1.437 on 23 degrees of freedom				
Multiple R-squared	0.975		Adjusted R-squared	0.9663	
F-statistic	112 on 8 and 23 DF		p-value	< 2.2e-16	
Significant code: 0 '***', 0.001 '**', 0.01 '*', 0.05 '.' 0.1-1 ' '					

The residual standard error is a measure of the model's fit to the data. A regression model's fit to a dataset improves as the residual standard error decreases. The larger the residual standard error, however, the less a regression model fits a dataset. A regression model with a low residual standard error will have variables clustered around the fitted regression line. In this case, the model's residual standard error is 1.437, implying that the regression model suggests the PCE of the PSC with an average error equivalent to approximately 1.437. Multiple R-squared is applied to display the proportion of PCE fluctuations explained by the eight input parameters. Basically said, it is a way for measuring the data-fitting capabilities of a constructed model. Multiple R-squared explains ~97.5% of the variation within PCE in this case. Adjusted R-squared is utilized when performing multiple linear regression and can be functionally compared to Multiple R-squared. The Adjusted R-squared indicates what proportion of the variation in PCE is explained by all predictors. The distinction between these two measures is a calculation subtlety that accounts for the PCE variation introduced by the addition of input parameters.

In this case, adjusted R-squared explains there is ~96.63% of the variation within PCE. Based on the constructed model, the F-statistic is quite large and the p-value is so small that it is effectively zero. This would suggest that the null hypothesis should be rejected leading to the conclusion that PCE and eight input parameters have a significant relationship. Thus, the objective function describing the relationship between PCE (the dependent variable) and eight input parameters (the independent variables) can be derived as:

$$PCE = 1.266e+01 - 1.068a + 1.248e-20b - 4.781c + 8.688e-22d + 1.794e+01e \\ 01e + 4.803e-20f - 7.396e-01g + 1.719e-21h \quad (2)$$

Theoretically, the Genetic algorithm is used to find for the minima of a function. Thus, the objective function in (2) was inverted to search for its local maxima. Subject to the fixed constraints, the fitness function of the maximizing purpose can be expressed as:

$$fi = -1.266e+01 + 1.068a - 1.248e-20b + 4.781c - 8.688e-22d - 1.794e+01e \\ 4.803e-20f + 7.396e-01g - 1.719e-21h \quad (3)$$

The fitness function (fi) is subjected repeatedly to the phases of selection, crossover, and mutation until its maximum value is found. As depicted in Figure 9, the process of selection, crossover, and mutation was terminated after 844 cycles.

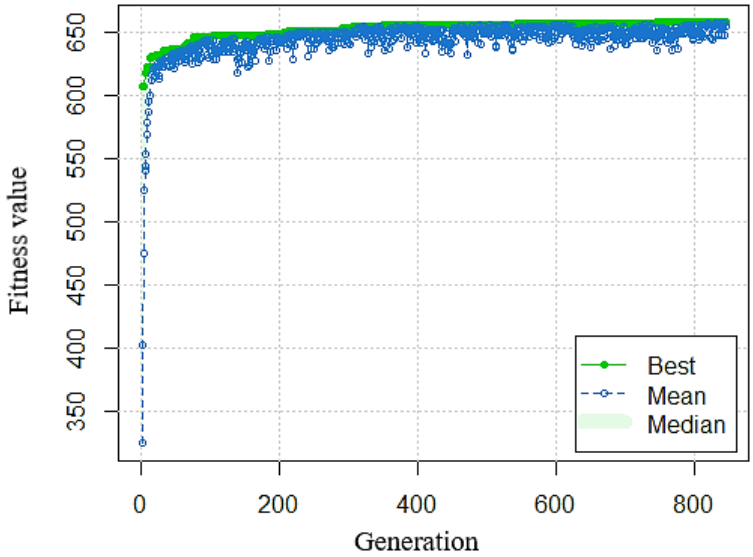

Fig. 9. Performance of Genetic algorithm during convergence

Based on the results of the Genetic algorithm, the largest achievable fitness value of the PCE is determined to be 657.64, where the optimal values of the input parameters; FTO thickness, FTO donor density, TiO_2 layer thickness, TiO_2 donor density, $CH_3NH_3PbI_{3-x}Cl_x$ layer thickness, $CH_3NH_3PbI_{3-x}Cl_x$ donor density, GO layer thickness, and GO acceptor density are predicted to be 0.187 µm, $9.965x10^{21}$ cm^{-3}, 0.033 µm, $9.629x10^{21}$ cm^{-3}, 0.926 µm, $9.983x10^{21}$ cm^{-3}, 0.039 µm and $9.671x10^{21}$ cm^{-3} respectively. For validation purpose, the Graphene-based PSC model is simulated again using the recently predicted input parameters via SCAPS-1D. Figure 10 depicts the comparison of J-V transfer characteristics PSC prior to optimization using L_{32} Taguchi DoE and L_{32} Taguchi DoE-based Genetic algorithm.

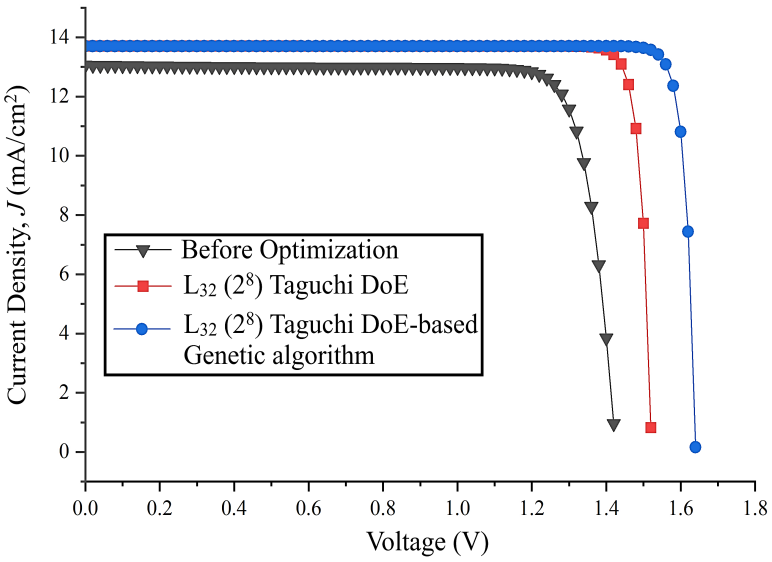

Fig. 10. Overlay of *J-V* transfer characteristics of the PSC before optimization, via Taguchi DoE and via L_{32} Taguchi DoE-based Genetic algorithm

Based on the overlay plot, the Voc of the PSC has increased by 13.4% after being optimized with the L_{32} Taguchi DoE-based Genetic algorithm compared to before optimization. In addition, the Voc demonstrates a 7.2% improvement over to the L_{32} Taguchi DoE approach, conducted using Minitab software [37]. The Jsc of the PSC after optimization using L_{32} Taguchi DoE-based Genetic algorithm has improved by 49.1%, with the Jsc before optimization approach and after L_{32} Taguchi DoE-based Genetic algorithm being 13.06 mA/cm^2 and 25.68 mA/cm^2, respectively. Jsc value skyrockets primarily as a result of enormous resistive losses brought on by large thickness variations in $CH_3NH_3PbI_{3-X}Cl_X$. However, there is no difference between the Jsc value and the L_{32} Taguchi DoE approach, where the Jsc remains unchanged at 25.68 mA/cm^2. Table 6 summarizes the input parameter values and simulation outcomes of the PSC.

Table 6
Summary of simulation outputs of the PSC

Symbol	Input parameter	Units	Before optimization (first experiment row)	L_{32} Taguchi DoE approach	L_{32} Taguchi DoE-based Genetic algorithm
a	FTO thickness	µm	0.1	0.1	0.187
b	FTO donor concentration	cm^{-3}	1x10^{11}	1x10^{20}	9.965x10^{21}
c	TiO_2 thickness	µm	0.03	0.03	0.033
d	TiO_2 donor concentration	cm^{-3}	1x10^{11}	1x10^{20}	9.629x10^{21}
e	$CH_3NH_3PbI_{3-X}Cl_X$ thickness	µm	0.1	0.9	0.926
f	$CH_3NH_3PbI_{3-X}Cl_X$ donor concentration	cm^{-3}	1x10^{11}	1x10^{20}	9.983x10^{21}
e	GO thickness	µm	0.03	0.03	0.039
h	GO acceptor concentration	cm^{-3}	1x10^{11}	1x10^{20}	9.671x10^{21}
Open voltage (Voc)		V	1.426	1.529	1.647
Current density (Jsc)		mA/cm^2	13.06	25.68	25.68
Fill factor (FF)		%	84.08	91.49	92.03
Power conversion efficiency (PCE)		%	15.66	35.91	38.93

According to Table 6, the PSC exhibits a 59.8% increase in PCE, with the PCE increasing from 15.66% to 38.93% upon optimization with the L_{32} Taguchi DoE-based Genetic algorithm. In addition, the FF is enhanced by 8.6% upon optimization with the L_{32} Taguchi DoE-based Genetic algorithm. In addition, it is also noticed that both FF and PCE have improved by 0.59% and 7.76%, respectively, compared to the optimization via the L_{32} Taguchi DoE approach. The simulated 38.93% of PCE is due to the use of heterojunction perovskite solar cells (PSCs), which differ greatly from single-junction solar cells. The Shockley-Queisser (SQ) limit, which defines the maximum theoretical efficiency for single-junction cells, does not restrict multi-junction or heterojunction cells. These advanced cells can surpass the SQ limit by utilizing multiple layers or junctions that absorb different segments of the solar spectrum more efficiently. The high efficiency of these PSCs is a result of their specialized structure and materials.

By optimizing the materials and cell configuration, researchers can substantially reduce losses and enhance light absorption, leading to efficiencies greater than those of traditional single-junction cells. For instance, recent developments in crystalline silicon-perovskite tandem solar cells have shown efficiencies up to 33.9% [38]. The simulated structure described in the study probably incorporates such innovative designs and materials to achieve the 38.93% efficiency. Furthermore, this impressive theoretical PCE is observed through simulations, and the actual PCE might differ when validated through experimental fabrication and testing. Hence, the final results demonstrate that the L_{32} Taguchi DoE-based Genetic algorithm could be applied to simulate solar cell devices effectively.

In future, the L_{32} Taguchi DoE could be incorporated with alternative approaches besides Genetic algorithm in an effort to provide more precise and inclusive solutions.

5. Conclusions

In summary, the optimum input parameters of the Perovskite solar cell device were accurately predicted using SCAPS-1D software integrated with L_{32} Taguchi DoE-based Genetic algorithm. This study's primary goal was to identify the input parameters of the device that would generate the maximum feasible power conversion efficiency (PCE). The thickness of $CH_3NH_3PbI_{3-X}Cl_X$ was deemed the most significant input parameter based on multiple linear regression analysis, as it had the lowest p-value among others. Subsequently, the objective function that links the eight input parameters with PCE was then statistically derived. The Genetic algorithm was employed to search the maximum converging point of the objective function within lower and upper specified boundaries. After 844 iterations, the highest fitness value (f_i) is determined to be 657.64. Using the anticipated optimum input parameters, the predicted model generated the highest possible PCE of 38.93%. The final findings imply that the L_{32} Taguchi DoE-based Genetic algorithm can be regarded as one of the effective methods in boosting the overall PSC's performance.

Acknowledgement

The authors would like to thank the Ministry of Higher Education (MOHE) for sponsoring this work under project (FRGS/1/2022/TK07/UTEM/02/47) and MiNE, CeTRI, Faculty of Electronics and Computer Technology and Engineering (FTKEK), Universiti Teknikal Malaysia Melaka (UTeM) for the moral support throughout the project.

Reference

[1] Salih, Mohammed Alamin, Mustafa Abbas Mustafa, and Bashria AA Yousef. "Developing lead-free perovskite-based solar cells with planar structure in confined mode arrangement using SCAPS-1D." *Sustainability* 15, no. 2 (2023): 1607. https://doi.org/10.3390/su15021607

[2] Hossain, M. Khalid, GF Ishraque Toki, Intekhab Alam, Rahul Pandey, D. P. Samajdar, Md Ferdous Rahman, Md Rasidul Islam, M. H. K. Rubel, H. Bencherif, Jaya Madane and Mustafa K. A. Mohammed. "Numerical simulation and optimization of a CsPbI 3-based perovskite solar cell to enhance the power conversion efficiency." *New Journal of Chemistry* 47, no. 10 (2023): 4801-4817. https://doi.org/10.1039/D2NJ06206B

[3] Chen, Qinmiao, Yi Ni, Xiaoming Dou, and Yamaguchi Yoshinori. "The effect of energy level of transport layer on the performance of ambient air prepared perovskite solar cell: A SCAPS-1D simulation study." *Crystals* 12, no. 1 (2022): 68. https://doi.org/ 10.3390/cryst12010068

[4] Sahoo, Arpita, Ipsita Mohanty, and Sutanu Mangal. "Effect of acceptor density, thickness and temperature on device performance for tin-based perovskite solar cell." *Materials Today: Proceedings* 62 (2022): 6210-6215. https://doi.org/ 10.1016/j.matpr.2022.05.095

[5] Mohanty, Ipsita, Sutanu Mangal, and Udai P. Singh. "Influence of defect densities on perovskite (CH3NH3PbI3) solar Cells: Correlation of experiment and simulation." *Materials Today: Proceedings* 62 (2022): 6199-6203. https://doi.org/ 10.1016/j.matpr.2022.05.090

[6] Hossain, M. Khalid, Mirza Humaun Kabir Rubel, GF Ishraque Toki, Intekhab Alam, Md Ferdous Rahman, and H. Bencherif. "Effect of various electron and hole transport layers on the performance of $CsPbI_3$-based perovskite solar cells: A numerical investigation in DFT, SCAPS-1D, and wxAMPS frameworks." *ACS omega* 7, no. 47 (2022): 43210-43230. https://doi.org/10.1021/acsomega.2c05912

[7] Riyad, Md Nur Hossain, Adil Sunny, Most Marzia Khatun, Sabrina Rahman, and Sheikh Rashel Al Ahmed. "Performance evaluation of WS2 as buffer and Sb2S3 as hole transport layer in CZTS solar cell by numerical simulation." *Engineering Reports* 5, no. 5 (2023): e12600. https://doi.org/10.1002/eng2.12600

[8] Hossain, M. Khalid, A. A. Arnab, Ranjit C. Das, K. M. Hossain, M. H. K. Rubel, Md Ferdous Rahman, H. Bencherif, M. E. Emetere, Mustafa KA Mohammed, and Rahul Pandey. "Combined DFT, SCAPS-1D, and wxAMPS frameworks for design optimization of efficient Cs 2 BiAgI 6-based perovskite solar cells with different charge transport layers." *RSC Advances* 12, no. 54 (2022): 35002-35025. https://doi.org/10.1039/D2RA06734J

[9] Kaharudin, K. E., F. Salehuddin, A. S. M. Zain, and Ameer F. Roslan. "Predictive analytics of CIGS solar cell using a combinational GRA-MLR-GA model." *Journal of Engineering Science and Technology* 15, no. 4 (2020): 2823-2840.
[10] Pochont, Nitin Ralph, Yendaluru Raja Sekhar, Kuraganti Vasu, and Rajan Jose. "Nitrogen-doped titanium dioxide as a hole transport layer for high-efficiency formamidinium perovskite solar cells." *Molecules* 27, no. 22 (2022): 7927. https://doi.org/ 10.3390/molecules27227927
[11] Abdulmalik, Muhammed O., Eli Danladi, Rita C. Obasi, Philibus M. Gyuk, Francis U. Salifu, Suleiman Magaji, Anselem C. Egbugha, and Daniel Thomas. "Numerical study of 25.459% alloyed inorganic lead-free perovskite CsSnGeI3-based solar cell by device simulation." *East European Journal of Physics* 4 (2022): 125-135. https://doi.org/10.26565/2312-4334-2022-4-12
[12] Salem, Marwa S., Ahmed Shaker, M. Abouelatta, Adwan Alanazi, Kawther A. Al-Dhlan, and Tariq S. Almurayziq. "Numerical analysis of hole transport layer-free antimony selenide solar cells: Possible routes for efficiency promotion." *Optical Materials* 129 (2022): 112473. https://doi.org/10.1016/j.optmat.2022.112473
[13] Kaharudin, Khairil Ezwan, and Fauziyah Salehuddin. "Predictive modeling of mixed halide perovskite cell using hybrid L_{27} OA Taguchi-based GA-MLR-GA approach." *Jurnal Teknologi* 84, no. 1 (2022): 1-9. https://doi.org/ 10.11113/jurnalteknologi.v84.15550
[14] Kaharudin, K. E., F. Salehuddin, A. S. M. Zain, M. N. I. A. Aziz, and I. Ahmad. "Application of Taguchi Method for Lower Subthreshold Swing in Ultrathin Pillar SOI VDGMOSFET Device." *Journal of Advanced Research in Applied Sciences and Engineering Technology* 2, no. 1 (2016): 30-43.
[15] Kaharudin, K. E., F. Salehuddin, and A. S. M. Zain. "Optimization of electrical properties in TiO2/WSix-based vertical DG-MOSFET using Taguchi-based GRA with ANN." *Journal of Telecommunication, Electronic and Computer Engineering (JTEC)* 10, no. 1 (2018): 69-76.
[16] Kaharudin, K. E., F. Salehuddin, A. S. M. Zain, and M. N. I. A. Aziz. "Application of Taguchi-based grey fuzzy logic for simultaneous optimization in TiO2/WSix-based vertical double-gate MOSFET." *Journal of Telecommunication, Electronic and Computer Engineering (JTEC)* 9, no. 2-13 (2017): 23-28.
[17] Kaharudin, K. E., F. Salehuddin, A. S. M. Zain, M. N. I. A. Aziz, Zahariah Manap, Nurul Akmal Abd Salam, and Wira Hidayat Mohd Saad. "Design and optimization of TiSi x/HfO 2 channel vertical double gate NMOS device." In *2016 IEEE International Conference on Semiconductor Electronics (ICSE)*, pp. 69-73. IEEE, 2016. https://doi.org/10.1109/SMELEC.2016.7573593
[18] AL-Jizani, Khalid Hammood, and Jawad Kadhim K. Al-Delfi. "An analytic solution for Riccati Matrix delay differential equation using coupled homotopy-Adomian approach." *Baghdad Science journal* 19, no. 4 (2022): 0800-0800. https://doi.org/10.21123/bsj.2022.19.4.0800
[19] AL-Jizani, Khalid Hammood. "A new technique of semi analytic approach α-Homo for obtaining the analytic solution to quadratic differential equations: Theory and applications." In *AIP Conference Proceedings* 2658, no. 1. AIP Publishing, 2022. https://doi.org/10.1063/5.0106904
[20] AL-Jizani, Khalid Hammood. "An efficient semi analytic technique for solving non-linear initial value problems." In *AIP Conference Proceedings*, vol. 2658, no. 1. AIP Publishing, 2022. https://doi.org/10.1063/5.0106903
[21] Al-jiz, Khalid Hammood, Noor Atinah Ahmad, and Fadhel Subhi Fadhel. "Variational iteration method for solving Riccati matrix differential equations." *Indonesian Journal of Electrical Engineering and Computer Science* 5, no. 3 (2017). http://doi.org/10.11591/ijeecs.v5.i3.pp673-683
[22] Mohammedali, Khalid Hammood, Noor Atinah Ahmad, and Fadhel S. Fadhel. "He's variational iteration method for solving Riccati matrix delay differential equations of variable coefficients." In *AIP Conference Proceedings*, 1830, no. 1. AIP Publishing, 2017. https://doi.org/10.1063/1.4980892
[23] Kaharudin, K.E., F. Salehuddin, Na Jalaludin, F. Arith, Asm Zain, I. Ahmad, and Sam Junos. "Predictive analytics of junctionless double gate strained mosfet using genetic algorithm with DoE-based grey relational analysis." *Journal of Engineering Science and Technology* 18, no. 6 (2023): 3077-3096.
[24] Bahrudin, M. S., Siti Fazlili Abdullah, and Ibrahim Ahmad. "Statistical modeling of solar cell using Taguchi method and TCAD tool." In *2012 10th IEEE International Conference on Semiconductor Electronics (ICSE)*, pp. 1-5. IEEE, 2012. https://doi.org/ 10.1109/SMElec.2012.6417073
[25] Oktiawati, Unan Yusmaniar, Norani Muti Mohamed, and Zainal Arif Burhanudin. "Applications of Taguchi method for optimization of dye solar cell design." *Sains Malaysiana* 46, no. 3 (2017): 503-508.
[26] Fadzilah, N., M. Z. A. A. Kadir, Suhaidi Shafie, S. A. Rashid, WZ Wan Hassan, and J. Norhanisah. "TiO_2 thickness and graphene quantum dots variation in photoanode of dye sensitized solar cell using response surface methodology (RSM) technique."*Solid State Science and Technology* 26, no. 2 (2018): 43-49.
[27] Bahrudin, Mohd Shaparuddin, Siti Fazlili Abdullah, Ibrahim Ahmad, Ahmad Wafi Mahmood Zuhdi, Azri Husni Hasani, Fazliyana Za'Abar, Mazin Malik, and M. Najib Harif. "J sc and V oc optimization of perovskite solar cell with interface defect layer using Taguchi method." In *2018 IEEE International Conference on Semiconductor Electronics (ICSE)*, p. 192-196. IEEE, 2018. https://doi.org/ 10.1109/SMELEC.2018.8481203

[28] Zapata-Cruz, J. R., Eddie N. Armendáriz-Mireles, E. Rocha-Rangel, G. Suarez-Velazquez, D. González-Quijano, and W. J. Pech-Rodríguez. "Implementation of Taguchi method to investigate the effect of electrophoretic deposition parameters of SnO_2 on dye sensitised solar cell performance." *Materials Technology* 34, no. 9 (2019): 549-557. https://doi.org/10.1080/10667857.2019.1591730

[29] Bahrudin, Mohd Shaparuddin, Yulisa Yusoff, Siti Fazlili Abdullah, Ahmad Wafi Mahmood Zuhdi, Nowshad Amin, and Ibrahim Ahmad. "An Innovative Parametric Optimization using Taguchi Method for Cu (In, Ga)(S, Se) 2 Thin Film Solar Cell Device Simulation." *Journal of Energy and Environment* (2020).

[30] Mohammed, Ayman R., and Irene S. Fahim. "Tandem organic solar cell optimization using response surface methodology." In *2020 International Conference on Data Analytics for Business and Industry: Way Towards a Sustainable Economy (ICDABI)*, pp. 1-5. IEEE, 2020. https://doi.org/10.1109/ICDABI51230.2020.9325624

[31] Abdelkadir, Abdelaziz Ait, Essaadia Oublal, Mustapha Sahal, and Alain Gibaud. "Numerical simulation and optimization of n-Al-ZnO/n-CdS/p-CZTSe/p-NiO (HTL)/Mo solar cell system using SCAPS-1D." *Results in Optics* 8 (2022): 100257. https://doi.org/10.1016/j.rio.2022.100257

[32] Olabi, Abdul Ghani, Hegazy Rezk, Mohammad Ali Abdelkareem, Tabbi Awotwe, Hussein M. Maghrabie, Fatahallah Freig Selim, Shek Mohammod Atiqure Rahman, Sheikh Khaleduzzaman Shah, and Alaa A. Zaky. "Optimal parameter identification of perovskite solar cells using modified bald eagle search optimization algorithm." *Energies* 16, no. 1 (2023): 471. https://doi.org/10.3390/en16010471

[33] Alla, Mohamed, Vishesh Manjunath, Najwa Chawki, Diwakar Singh, Subhash C. Yadav, Mustapha Rouchdi, and Fares Boubker. "Optimized CH3NH3PbI3-XClX based perovskite solar cell with theoretical efficiency exceeding 30%." *Optical Materials* 124 (2022): 112044. https://doi.org/10.1016/j.optmat.2022.112044

[34] Touafek, N., R. Mahamdi, and C. Dridi. "Boosting the performance of planar inverted perovskite solar cells employing graphene oxide as HTL." *Digest Journal of Nanomaterials and Biostructures* 16, no. 2 (2021): 705-712.

[35] Mombeshora, Edwin T., Edigar Muchuweni, Rodrigo Garcia-Rodriguez, Matthew L. Davies, Vincent O. Nyamori, and Bice S. Martincigh. "A review of graphene derivative enhancers for perovskite solar cells." *Nanoscale Advances* 4, no. 9 (2022): 2057-2076. https://doi.org/10.1039/D1NA00830G

[36] Nowsherwan, Ghazi Aman, Abdul Samad, Muhammad Aamir Iqbal, Tauqeer Mushtaq, Ameer Hussain, Maria Malik, Sabah Haider, Phuong V. Pham, and Jeong Ryeol Choi. "Performance analysis and optimization of a PBDB-T: ITIC based organic solar cell using graphene oxide as the hole transport layer." *Nanomaterials* 12, no. 10 (2022): 1767. https://doi.org/10.3390/nano12101767

[37] Kaharudin, Khairil E., Nabilah A. Jalaludin, Fauziyah Salehuddin, Faiz Arith, Anis SM Zain, Ibrahim Ahmad, Siti AM Junos, and Abdul H. Afifah Maheran. "Optimal modeling of perovskite solar cell with graphene oxide as hole transport layer using L32 (28) Taguchi design." *International Journal of Nanoelectronics and Materials (IJNeaM)* 17, no. 1 (2024): 20-27. https://doi.org/10.58915/ijneam.v17i1.448

[38] Kumar, Prasun, Swetha Thokala, Surya Prakash Singh, and Ranbir Singh. "Research progress and challenges in extending the infra-red absorption of perovskite tandem solar cells." *Nano Energy* 121 (2024): 109175. https://doi.org/10.1016/j.nanoen.2023.109175